Cell, Vol. 101, 671–684, June 9, 2000, Copyright ©2000 by Cell Press

Drosophila Dscam Is an Axon Guidance Receptor Exhibiting Extraordinary Molecular Diversity

Dietmar Schmucker,*§ James C. Clemens,*†§ Huidy Shu,*§ Carolyn A. Worby,† Jian Xiao,* Marco Muda,† Jack E. Dixon,†‡ and S. Lawrence Zipursky*‡
*Howard Hughes Medical Institute
Department of Biological Chemistry
UCLA School of Medicine
675 Charles E. Young Dr. South
Los Angeles, California 90095
†University of Michigan
Department of Biological Chemistry
1301 E. Catherine
Ann Arbor, Michigan 48109

Summary

A *Drosophila* homolog of human Down syndrome cell adhesion molecule (DSCAM), an immunoglobulin superfamily member, was isolated by its affinity to Dock, an SH3/SH2 adaptor protein required for axon guidance. Dscam binds directly to both Dock's SH2 and SH3 domains. Genetic studies revealed that Dscam, Dock and Pak, a serine/threonine kinase, act together to direct pathfinding of Bolwig's nerve, containing a subclass of sensory axons, to an intermediate target in the embryo. Dscam also is required for the formation of axon pathways in the embryonic central nervous system. cDNA and genomic analyses reveal the existence of multiple forms of Dscam with a conserved architecture containing variable Ig and transmembrane domains. Alternative splicing can potentially generate more than 38,000 Dscam isoforms. This molecular diversity may contribute to the specificity of neuronal connectivity.

Introduction

Classical embryological, genetic, and biochemical approaches have led to important insights into the mechanisms by which neurons form connections during development (Lance-Jones and Landmesser, 1981; Thomas et al., 1984; Goodman and Shatz, 1993). In both vertebrates and invertebrates, axon pathways are established in a stepwise fashion. The growth cone, a sensorimotor structure at the leading edge of the extending axon, detects specific signals and translates them into directed movement (Lin and Forscher, 1993; Tanaka and Sabry, 1995). Growth cones migrate through complex cellular environments by responding to specific guidance cues produced by cells along their trajectories. Once in the target region, growth cones stop, select specific targets, and form synapses. In some regions of the nervous system, these connections are further modified by neuronal activity (reviewed by Albright et al., 2000).

Extraordinary progress has been made in identifying guidance signals and their receptors. These signals may be secreted or membrane-bound and they can attract or repel growth cones (Tessier-Lavigne and Goodman, 1996; Culotti and Merz, 1998; Guthrie, 1999). The response of a growth cone to specific signals is determined by the receptors on its surface and the activity of signaling pathways acting within the growth cone (Ming et al., 1997; Bashaw and Goodman, 1999; Hong et al., 1999). Connection specificity requires growth cones to respond to different levels of the same signal (Flanagan and Vanderhaeghen, 1998) and combinations of different signals (Winberg et al., 1998), to integrate this information, and to translate it into changes in motility (Suter and Forscher, 1998). While it is clear that these events must ultimately converge on the actin-based cytoskeleton of the motility apparatus in the growth cone, the biochemical mechanisms by which this occurs are not well understood.

To gain insight into the mechanisms by which growth cones integrate guidance cues, we pursued a combined biochemical and genetic analysis of the Dock signal transduction pathway. Dock is an adaptor protein containing 3 SH3 domains and a single SH2 domain, and is closely related to mammalian Nck (Clemens et al., 1996; Garrity et al., 1996; Rao and Zipursky, 1998). *dock* mutants show defects in axon guidance in the adult fly visual system (Garrity et al., 1996) and in the embryonic nervous system (Desai et al., 1999). Based on the role of the adaptor protein Grb-2 in linking receptor tyrosine kinases to Ras (Olivier et al., 1993), we proposed that Dock links guidance receptors to downstream regulators of the actin cytoskeleton. We previously demonstrated that Pak, a p21-activated serine/threonine kinase, acts downstream of Dock in adult photoreceptor neurons (Hing et al., 1999). Dock binds through its second SH3 domain to Pak and Pak binds directly to Rho family GTPases (Manser et al., 1994), evolutionarily conserved regulators of the actin-based cytoskeleton (Nobes and Hall, 1995; Hall, 1998). Genetic studies revealed that both Pak's kinase activity and its interaction with Rho family GTPases are essential for axon guidance (Hing et al., 1999).

In this paper, we describe a novel guidance receptor that is highly related to a human protein called Down syndrome cell adhesion molecule (Yamakawa et al., 1998; see Discussion). *Drosophila* Dscam was identified in a novel screen for proteins interacting with the Dock SH2 domain. Dscam binds directly to multiple domains of Dock and is widely expressed on axons in the embryonic nervous system. To gain insight into the mechanism by which Dscam, Dock, and Pak function in growth cones, we focused on their roles at a single guidance step in the simple axon trajectory of Bolwig's nerve (BN) in the embryo. We show that Dscam is required for recognition of an intermediate targeting determinant for the BN, that Dock and Pak are required for this step, and that *Dscam* shows dosage-sensitive interactions

‡To whom correspondence should be addressed (e-mail: zipursky@hhmi.ucla.edu [S. L. Z.], jedixon@umich.edu [J. E. D.]).
§These authors contributed equally to this work.

with both *dock* and *Pak*. Based on these studies, we propose that Dscam recognizes a guidance signal(s) and translates it into changes in the actin-based cytoskeleton through Dock and Pak.

In the course of the analysis of Dscam cDNAs, we uncovered extraordinary sequence diversity in the extracellular region. Through splicing of alternative exons encoding three different Ig domains and the transmembrane domain, more than 38,000 proteins may be generated. These proteins would have an identical architecture but differ in their combination of the four variable domains. We also show that Dscam is required in other neurons in the developing central nervous system for the establishment of axon pathways. This raises the intriguing possibility that diverse forms of a single protein may contribute to specifying the precise connections made by many different types of neurons.

Results

Identification of Dscam as a Dock-Interacting Protein

We reasoned that the Dock SH2 domain could be used as an affinity reagent to purify upstream guidance receptors in the Dock signaling pathway. Two tyrosine-phosphorylated proteins, p145 and p270, were detected in Dock immunoprecipitates of S2 cell extracts (Clemens et al., 1996). To obtain a source of cells from which to purify sufficient quantities of these proteins for microsequencing, we created an S2 cell line, $S2^{HisSH2}$, in which a histidine-tagged Dock SH2 domain (Figure 1A) was constitutively expressed. A dramatic increase in the level of phosphotyrosine in p145 and p270 was observed which may reflect protection from endogenous phosphatases by binding to the excess Dock-SH2 domain expressed in these cells (Figures 1B and 1C).

As a first step to purifying proteins associated with the Dock-SH2 domain, lysates prepared from $S2^{HisSH2}$ cells were subjected to Ni-agarose affinity chromatography (see Experimental Procedures). Tyrosine phosphorylated proteins corresponding to p145 and p270 copurified with the SH2 domain (compare Figures 1B and 1C). In addition, several other tyrosine-phosphorylated proteins, not previously detected in Dock immunoprecipitates, copurified (Figure 1D). These proteins were bound to a P-Tyr-specific antibody affinity column, eluted, and separated by SDS-PAGE electrophoresis. Coomassie-stained proteins with molecular weights of 270, 145, 74, 69, and 63 kDa were observed (Figure 1D). Here we focus on a biochemical and genetic analysis of p270. Detailed characterizations of the other proteins will be described elsewhere.

To obtain amino acid sequences of p270, the band was excised from the Coomassie-stained gel and digested with trypsin. Tryptic peptides were eluted and seven peptide sequences were determined. Two expressed sequence tags (ESTs) were identified that encoded all seven peptides. A 7,754 bp contig was assembled from ESTs and 5′ RACE products. This cDNA size is consistent with the 8 kb mRNA observed by Northern blot analysis (data not shown). The cDNA contains an open reading frame of 6,048 nucleotides encoding from

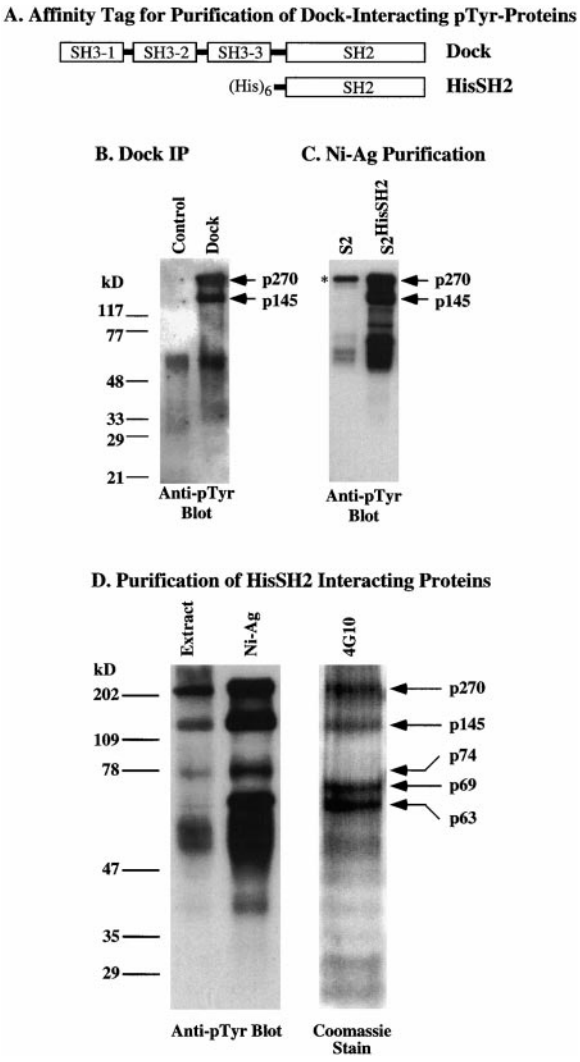

Figure 1. Identification and Isolation of Dock SH2 Domain–Associated Proteins

(A) Schematic representation of Dock and the SH2 domain of Dock modified with six tandemly arranged histidine residues at its N terminus (HisSH2).

(B) Tyrosine-phosphorylated (pTyr) proteins associated with Dock. Dock immunoprecitates from S2 cells were Western blotted with anti-phosphotyrosine antibody 4G10. Control is from immunoprecipitates using preimmune serum.

(C) Dock SH2 domain–associated proteins. pTyr-containing proteins from S2 cell extracts that express HisSH2 ($S2^{HisSH2}$) or vector controls (S2) were detected as in (B). The band labeled with an asterisk is of similar size to p270 and is of unknown identity. The X-ray film exposure time was 10-fold less in (C) than (B), indicating a strong enhancement of tyrosine phosphorylation of these proteins.

(D) Purification of pTyr-containing proteins. pTyr-containing proteins were purified from $S2^{HisSH2}$ by sequential binding to Ni-agarose and 4G10 affinity columns. Bound fractions from these columns are shown as indicated. As a final step in purification, proteins were separated by SDS-PAGE and identified by Coomassie stain. p74 is not visible as a Coomassie-stained band in this figure, but is visible in the pTyr blot in the Ni-agarose eluate. p69 is visible in the Coomassie-stained gel, but does not correspond to any pTyr-containing bands. Presumably this band is associated with a pTyr-containing protein that associates with the SH2 domain. Bands were excised, trypsin-treated, and microsequenced (see Results and Experimental Procedures).

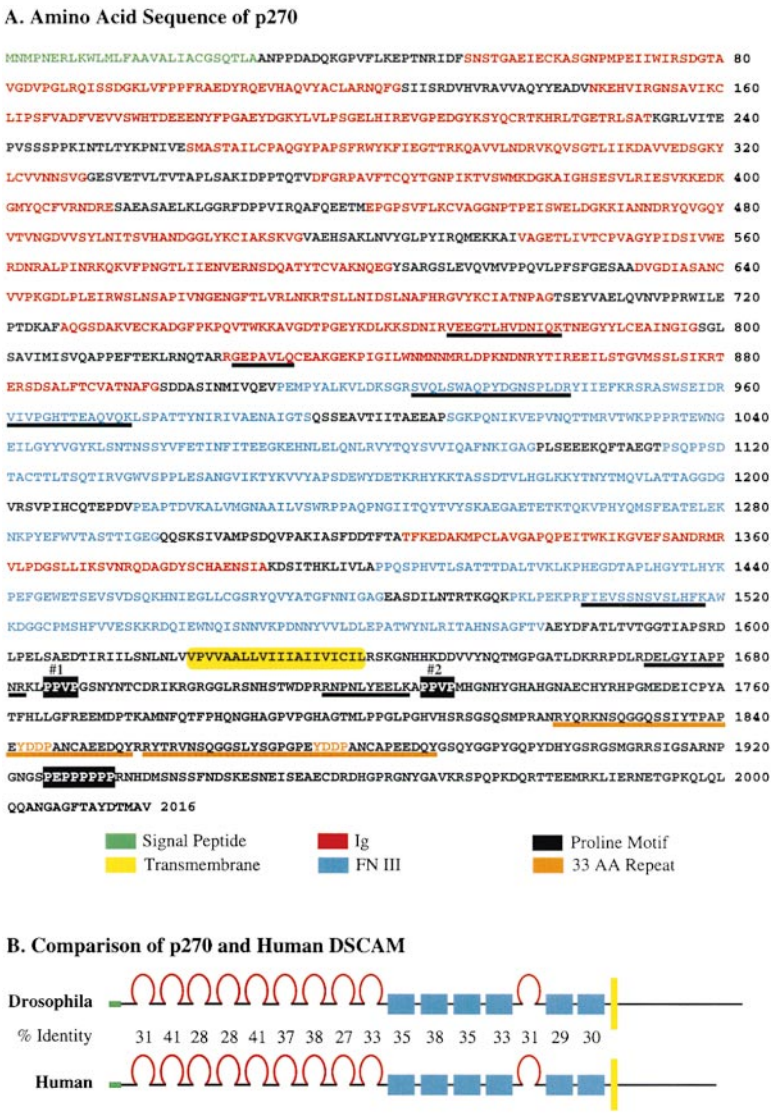

Figure 2. p270 Is *Drosophila* Dscam

(A) The amino acid sequence of p270. p270 is a single pass transmembrane protein containing multiple domains. These are color-coded as indicated. The amino acid sequences obtained for the p270 tryptic peptides are underlined. Two 33 amino acid direct repeats each contain a single Dock SH2-domain consensus binding site (YDDP). The PXXP motifs are numbered.

(B) The domain structures of p270 and human DSCAM are compared. Numbers between the schematics indicate percent identities between the compared domains. Based on the similarities in domain structure and amino acid sequence, we refer to p270, henceforth, as *Drosophila* Dscam (see text).

its N terminus as predicted from SMART analysis (Schultz et al., 2000) (Figure 2): (1) a putative signal peptide; (2) nine tandemly repeated immunoglobulin (Ig) domains; (3) four fibronectin type III (FNIII) domains; (4) a single Ig domain; (5) an additional two FNIII domains; (6) a transmembrane domain; and (7) a novel cytoplasmic domain of 374 amino acids containing multiple potential tyrosine phosphorylation sites and several putative SH3 binding sites. Interestingly, two 33 amino acid repeats are found in the cytoplasmic domain each containing a consensus Dock/Nck SH2 binding motif (Song et al., 1998; Stein et al., 1998).

The extracellular region of p270 contains Ig and FNIII domains that are frequently found in axon guidance receptors, including Robo (Kidd et al., 1998) and the netrin-receptor Frazzled (Kolodziej et al., 1996). p270 is most highly related to human *DSCAM*, a gene that has been implicated in the mental retardation associated with Down syndrome (Yamakawa et al., 1998). The number and organization of the extracellular domains of the fly and human proteins are identical. They share 32% sequence identity and 49% sequence similarity (Figure 2). In contrast, the intracellular domains appear unrelated (see Discussion). Based on the similarities in the extracellular domain, we refer to p270 as *Drosophila* Dscam.

Two lines of evidence indicate that p270 is Dscam (Figure 3A): (1) tyrosine phosphorylated p270 is depleted from S2 cells treated with Dscam double-stranded RNA (RNAi) (for use of RNAi in *Drosophila* S2 cells, see Clemens et al., 2000); (2) anti-Dscam antibody recognizes a band at 270 kDa that is missing in Dscam RNAi-treated S2 cells. Dscam is detected in Dock immunoprecipitates prepared from embryonic extracts (Figure 3B), where it also appears to be tyrosine phosphorylated. A second band, not seen in S2 cells, migrating at 220 kDa was detected by anti-Dscam and anti-pTyr. This may represent a cross-reactive protein. Alternatively, as the predicted molecular weight of Dscam after cleavage of the signal peptide is 219 kDa, this may reflect differences in posttranslational modification of Dscam.

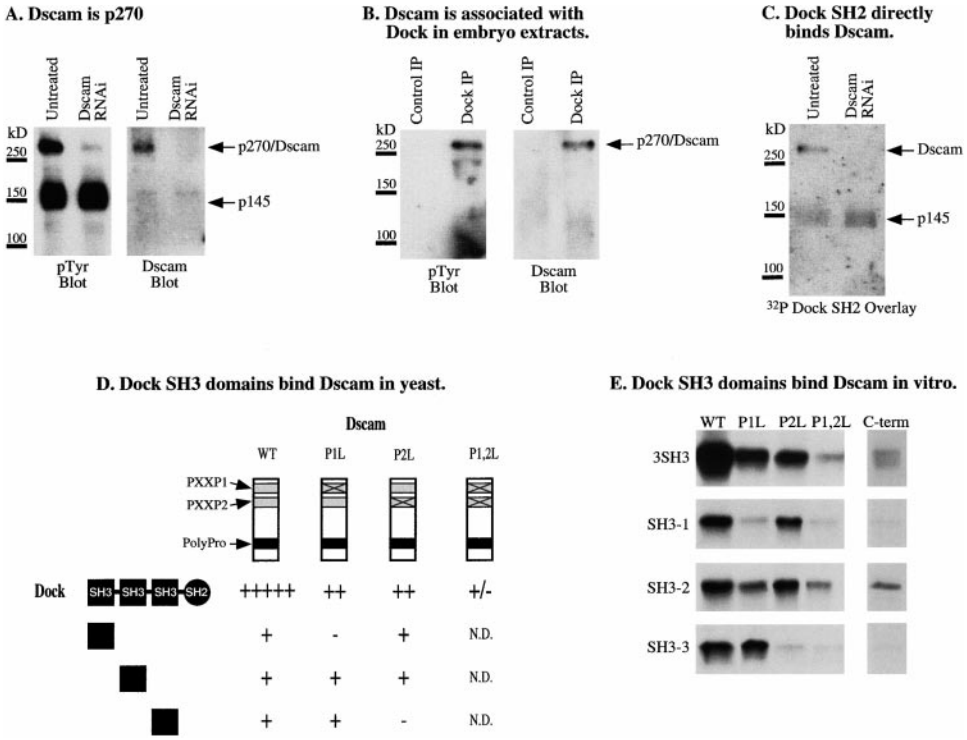

Figure 3. Dscam Binds to the SH2 and SH3 Domains of Dock

(A) Dscam is p270. The HisSH2 domain was purified from $S2^{HisSH2}$ cells (untreated) or $S2^{HisSH2}$ cells grown in the presence of Dscam double-stranded RNA (RNAi). HisSH2 domain–associated proteins were analyzed by immunoblotting with pTyr or Dscam antibodies as indicated. Tyrosine-phosphorylated p270 is greatly diminished in the Dscam RNAi lane while p145 is unaffected. Dscam immunoreactivity is not detected in Dscam RNAi cells.

(B) Dscam is associated with Dock in embryo extracts. Dock immunoprecipitates from 12–18 hr embryo extracts were analyzed by blotting with pTyr or Dscam antibodies as indicated. In addition to Dscam, which migrates at 270 kDa, a second band of 220 kDa is observed. The difference in size may reflect a posttranslational modification. Alternatively, p220 may be a cross-reactive band. The 270 kDa band is more heavily tyrosine phosphorylated as shown in the anti-pTyr blot.

(C) Dock SH2 directly binds Dscam. Dock immunoprecipitates from untreated or Dscam RNAi–treated S2 cells were probed with radiolabeled Dock SH2 domain. A band corresponding to Dscam was depleted by Dscam RNAi treatment. SH2 binding to p145 was detected in both lanes.

(D) Dock SH3 domains bind Dscam in yeast. Full-length Dock and individual SH3 domains fused to LexA were tested for interaction with wild-type or mutant Dscam cytoplasmic domains fused to Gal4 activation domain. The two PXXP sites and the polyproline motifs are represented by shaded and black boxes, respectively. Mutations in the PXXP motifs are indicated by Xs. The relative strengths of the interactions are represented by using "+" and "−" (see Experimental Procedures).

(E) Dock SH3 domains bind to Dscam in vitro. GST fused to the three SH3 (3SH3) domains together or each SH3 domain separately were tested for binding to wild-type and mutant forms of the cytoplasmic domain of Dscam synthesized in vitro (see Experimental Procedures). In addition to the forms of Dscam analyzed in (D), binding to a C-terminal fragment containing the polyproline motif also was tested.

The Cytoplasmic Domain of Dscam Interacts with Multiple Domains in Dock

We previously proposed that Dock interacts with upstream guidance signals in a redundant fashion through both SH3 and SH2 domains based on mutational analyses of domain requirements for Dock in axon guidance (Rao and Zipursky, 1998). The Dock SH2 domain interacts directly with Dscam as shown in a GST-SH2 domain gel overlay experiment (Figure 3C). Dock immunoprecipitates from S2 cells were separated on an SDS polyacrylamide gel and blotted with ^{32}P-labeled Dock SH2 domain. A tyrosine-phosphorylated band comigrating with Dscam bound to the radiolabeled probe (Figure 3C). Binding was disrupted by pretreatment with alkaline phosphatase (data not shown). That this band corresponds to Dscam is supported by the finding that it was missing in extracts prepared from S2 cells depleted of Dscam by RNAi.

The SH3 domains of Dock also directly interact with Dscam. Interactions between different SH3 domains and Dscam were assessed in a yeast two-hybrid assay and in GST pulldown experiments. In yeast, full-length Dock interacts strongly with the cytoplasmic domain of Dscam (Figure 3D). Each of the three SH3 domains tested individually in yeast showed reduced interaction. The SH3 domains also were shown to interact with the cytoplasmic domain of Dscam in GST pulldown experiments (Figure 3E). Dscam was bound by GST fused to the three SH3 domains (GST-3-SH3). While Dscam bound to each SH3 domain fused separately to GST, the fraction bound was considerably reduced when compared to GST-3-SH3. The amounts of GST fusion proteins used in these experiments were similar. This suggests Dock interacts through multiple SH3 domains with Dscam.

The interaction sites between different SH3 domains

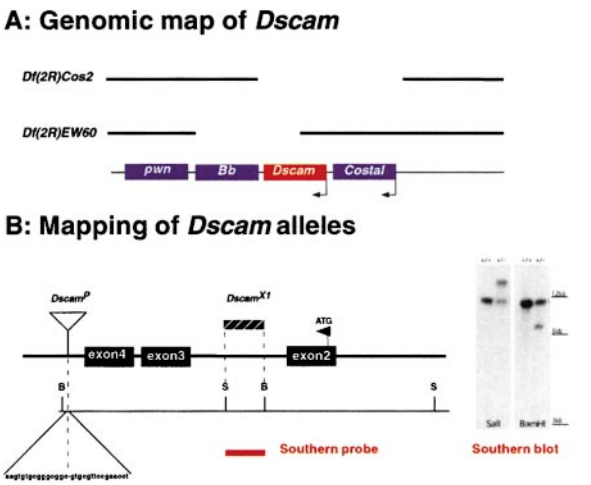

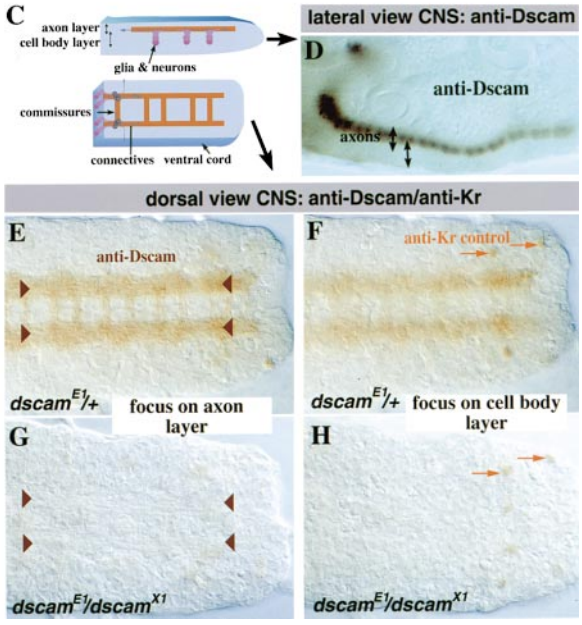

Figure 4. Dscam Protein Is Not Detected in *Dscam* Mutant Embryos

(A) *Dscam* maps to 43B1-4. Small chromosomal deficiencies in the 43B region are shown. Gaps correspond to deleted DNA.

(B) $Dscam^{P}$ is caused by P element insertion P05518. Sequence analysis revealed that the P element is located downstream of exon 4.1 (see Figure 8A). $Dscam^{X1}$ breaks between exons 2 and 3. Exon 2 contains the start ATG and part of the signal peptide.

(C–H) Dscam is expressed on axons in the embryonic CNS. (C) Schematics of CNS axon tracts. (D) Lateral view of anti-Dscam stained embryo. Staining is confined to the axon layer. (E and F) Axon tracts in *Dscam* heterozygotes stained with anti-Dscam (arrowheads). (G and H) No Dscam immunoreactivity is seen in homozygous *Dscam* embryos. As an internal control for staining, both homozygous and heterozygous embryos were costained with anti-Krueppel, a marker for a subset of neuronal nuclei (arrows).

and Dscam were mapped (Figures 3D and 3E). Two putative SH3 binding sites (PXXP1 and PXXP2) separated by 40 amino acids were found in the N-terminal portion of the Dscam cytoplasmic domain; a C-terminal polyproline sequence (PEPPP) also was found. Site-directed mutagenesis of the PXXP sites revealed that the first SH3 domain (SH3-1) binds preferentially to PXXP1 and third SH3 domain (SH3–3) to PXXP2 (see Figures 3D and 3E). GST-SH3-1 and GST-SH3-3 interact with the N-terminal half of the cytoplasmic tail of Dscam containing the PXXP sites, but only weakly to the C-terminal half encompassing the polyproline sequence. Conversely, the second SH3 domain (SH3-2) binds preferentially to the C-terminal polyproline motif. That PXXP1 and PXXP2 sequences are the primary interaction sites between Dock and Dscam is strongly supported by the marked reduction in interaction between Dock and the cytoplasmic domain of Dscam carrying point mutations in both these sites. Residual binding may be due to interaction between SH3-2 and the C-terminal polyproline sequence (Figure 3E). In summary, these data indicate that Dscam binds directly to Dock through both SH3 and SH2 domains, consistent with genetic studies arguing for redundancy between these domains.

Identification of *Dscam* Mutants

To critically assess whether *Dscam* is required for axon guidance, we sought to identify loss-of-function mutations. *Dscam* was localized to region 43B1-B3 by in situ hybridization to salivary gland polytene chromosomes. Four lethal complementation groups were previously mapped to this region by Heitzler et al. (1993) (Figure 4A). Sequences abutting a P element lethal insertion into one of these complementation groups, *l(2)43Bc,* were identical to sequences in a P1 genomic clone containing *Dscam* sequences. This insertion mapped 1200 nucleotides downstream from exon 4.1 (see section below and Figure 7 for genomic organization); exon 4 encodes part of the second Ig domain (Figure 4B). Two inversion alleles of *l(2)43Bc* also break within the *Dscam* locus. *In(LR)43b71kIA* breaks in the 8.8 kb intron separating exons 2 and 3 (Figure 4B). A second inversion, *In(2R)DX8*, also breaks within the *Dscam* locus, although the precise breakpoint was not identified. A single EMS allele, $l(2)43Bc^{1}$, fails to complement the inversions and the P allele. All alleles were early larval lethal. We have renamed them as follows: $l(2)43Bc^{1} = Dscam^{E1}$; *In(LR)43b71kIA* = $Dscam^{X1}$; *In(2R)Dx8* = $Dscam^{X2}$; and the P allele = $Dscam^{p}$.

To assess the effect of these mutations on Dscam protein expression, mutant embryos were stained with an antibody generated to an N-terminal peptide of Dscam. In wild type, Dscam staining is largely confined to axons in stage 16 embryos. Staining is most prominent in the connectives and the commissures (Figures 4C–4H). Dscam immunoreactivity was not detected in embryos homozygous for any of these alleles. The highly restricted expression of Dscam to axons suggested that it might play a direct role in axon guidance.

Axon Pathways in the Central Nervous System Are Disrupted in *Dscam* Mutants

As *Dscam* mutants are early larval lethal and Dscam is expressed on many axons in the developing embryonic CNS, we set out to assess whether mutations in *Dscam*

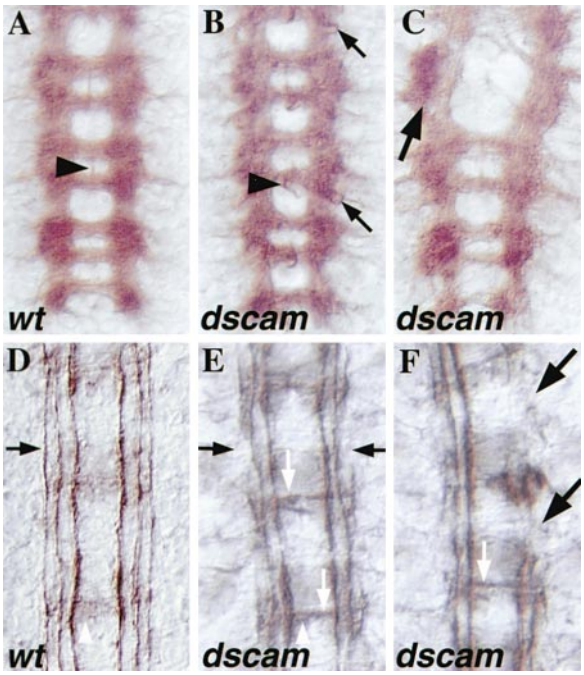

Figure 5. *Dscam* Disrupts Axon Tracts in the Embryo

(A–C) The CNS of stage 16 embryos stained with BP102. (A) The regular ladder-like pattern of stained connectives and commissures is seen in wild type. (B and C) Examples of weak and strong phenotypes in *Dscam* mutants, respectively. (B) Projections of the VUM neurons are abnormal (arrowhead; see [A] for wild type). (C) Disruption of commissures and irregularities in the thickness of the longitudinal tracts is observed (arrow).

(D–F) The CNS of stage 16 embryos stained with anti-Fas II (mAb1D4). (D) Continuous staining of three longitudinal axon tracts (arrow) on either side of the midline is observed in wild type. No FasII-labeled axon bundles cross the midline (white arrowhead). (E and F) Examples of weak and strong phenotypes in *Dscam* mutants, respectively. (E) The outer two fascicles are disrupted (black arrows) and abnormal crossing of the midline is observed (white arrows). In (F), massive disruption in these longitudinal tracts is observed (black arrow).

disrupt axon pathways. Axon tracts in stage 16 embryos were visualized with mAbBP102 (Figures 5A–5C) and mAb1D4 (Figures 5B–5D) an antibody to Fasciclin II. In wild-type embryos, mAbBP102 stains in a ladder-like pattern within the ventral nerve cord, highlighting the connectives and commissures. *Dscam* mutant embryos exhibit mild (Figure 5B) to severe (Figure 5C) disorganization of these tracts. mAb1D4 stains three continuous fascicles on both sides of the midline (Figure 5D). In *Dscam*, breaks in the connectives, predominantly of the outer two fascicles, were observed. Defects exhibited variable expressivity (Figures 5E and 5F). In addition, axon bundles aberrantly crossed the midline. These defects were seen in all embryos of two different heteroallelic combinations ($Dscam^{P}/Df$ and $Dscam^{E1}/Df$).

Dscam Is Required at a Specific Step in Bolwig's Nerve Axon Guidance

To gain insight into Dscam's role in guidance at a defined choice point for which both Dock and Pak also are required, we focused on Dscam's role in BN axon guidance. The projection of BN elaborates a simple and well-studied pathway (Schmucker et al., 1997). Bolwig's organ, a larval photosensitive structure, contains 12 photoreceptor neurons that extend a single bundle of axons during embryogenesis to their targets in the brain. BN extends posteriorly along the embryonic optic stalk to the surface of the optic lobe (see Schmucker et al., 1997). It then grows across the surface of the optic lobe to a presumptive intermediate target neuron, P2. At P2, the growth cones pause before projecting to their synaptic targets in the brain (see schematic in Figure 6). Phenotypes can be readily assessed in embryos double-stained for BN and P2, using mAb22C10 and anti-Bsh (brain-specific homeobox protein), respectively (Figure 6).

In stage 16 embryos carrying $Dscam^{E1}$ or $Dscam^{P}$ over a deficiency, some 53%–58% of BN projections were defective (n = 349; Table 1). In half of the "abnormal projections" the entire nerve mistargets, whereas in the remainder only a subset of axons does. Mistargeting axons either project past P2 or stop prematurely. Many of the projections scored as wild type, however, show abnormal expansion of BN terminus at P2. These guidance defects are unlikely to reflect an indirect consequence of defects in Bolwig's organ differentiation, as organ and cellular morphology in *Dscam* mutants were indistinguishable from wild type (data not shown). BN guidance phenotypes in *Dscam* mutants were similar to those seen in *dock* (n = 246) and *Pak* (n = 89) mutants (Figure 6; Table 1). The penetrance of *dock* and *Pak* were higher (90%–96%) than in *Dscam* (53%–58%). The incomplete penetrance of *Dscam* may reflect residual function due to maternal contribution. Alternatively, this may reflect redundancy as we have identified two additional genes encoding Dscam-related proteins in the fly genome (data not shown).

Dscam RNA is expressed in Bolwig's organ (Figure 6K) as well as more generally within the CNS and PNS (data not shown). The protein product is exclusively expressed on axon processes (see Figures 4D and 4E). To assess whether expression of Dscam selectively in BN was sufficient to rescue the mutant, we constructed a transgene encoding full-length Dscam driven by the GMR promoter (a strong transcriptional driver providing Bolwig's organ-specific expression) and introduced it into the germline by P element DNA transformation. Two independent insertions were characterized. In a wild-type (or a *Dscam* mutant) background, 100% of the embryos carrying one or two copies of GMR-*Dscam* exhibited strong axon guidance phenotypes (Figures 6L–6O). Individual axons projected in abnormal directions over the surface of the optic lobe and rarely contacted P2 (Figures 6N and 6O). It is unclear whether this reflects sensitivity of BN guidance to increased levels of Dscam or misexpression in Bolwig's organ of an inappropriate isoform (see below), or both. Due to the large size of the *Dscam* locus (61 kb), we were unable to assess whether the wild-type gene rescues the mutant phenotype. In any case, the dominant phenotype precluded assessing transgene rescue of the mutant phenotype. In contrast, GMR-*dock* rescued 85% of *dock* mutant embryos (Table 1; Figure 6B).

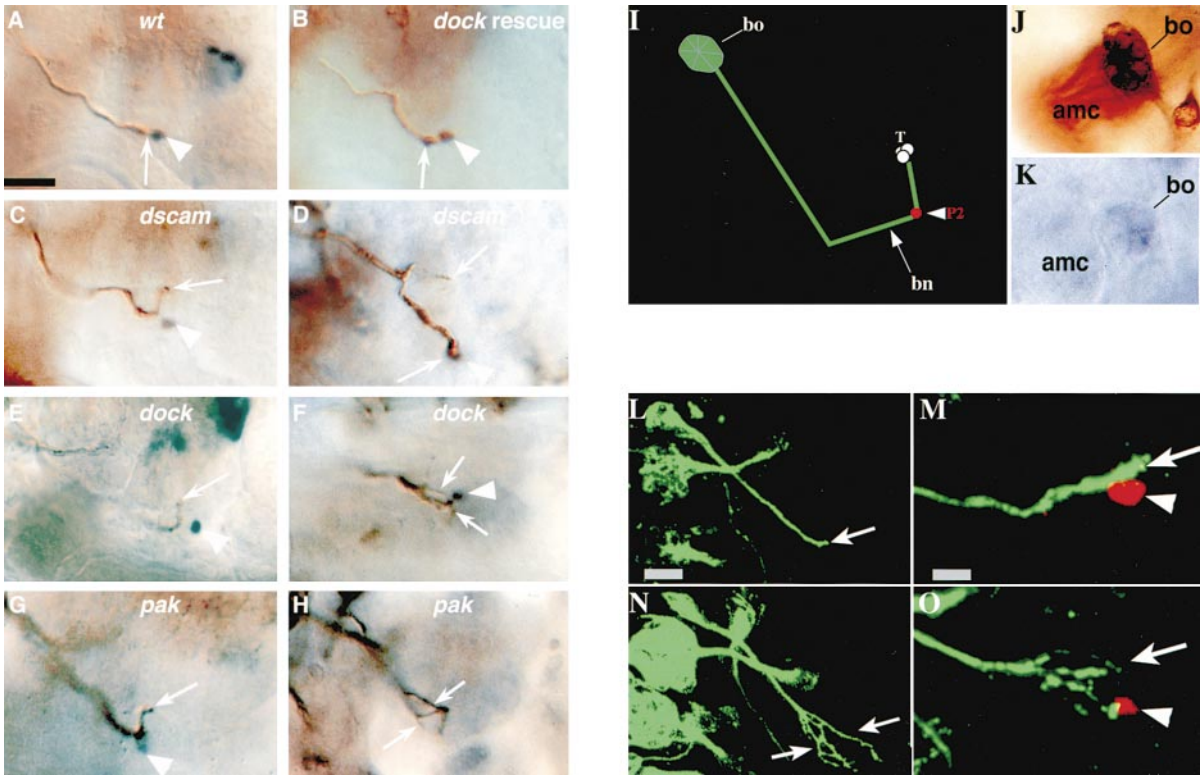

Figure 6. *Dscam*, *dock*, and *Pak* BN Axon Guidance Phenotypes Are Similar

(A–H) The BN projection in stage 16 wt and mutant embryos. BN stained with mAb22C10 (brown) and anti-Bsh (black; P2). (A) BN (arrow) projects with high accuracy to P2 (arrowhead). In *Dscam* (C and D), *dock* (E and F) and *Pak* (G and H) mutant embryos either the entire BN (C, E, and G) or a subset of axons (D, F, and H) project to ectopic positions (arrows). (B) A *dock* cDNA specifically expressed in BO by the GMR driver (see text) rescues the *dock* mutant phenotype. Genotypes: (C and D) $Dscam^{P}/Df(2R)cos\text{-}2$; (E), $dock^{P1}/dock^{P2}$; (F). $dock^{3}/dock^{3}$; (G and H) Pak^{6}/Pak^{11}. For quantitation see Table 1. (I) Schematic represention of the trajectory of the BN. The intermediate target P2 and the postsynaptic targets (T) in the brain are shown. (J) Indicates mAb22C10 staining showing characteristic rosette shape of Bolwig's organ (bo) located dorsal to the antennal maxillary complex (amc). (K) Expression of Dscam RNA in bo. (L–O) Overexpression of Dscam leads to a dominant phenotype in BN pathfinding. (L and N) Low magnification views of BN stained with mAb22C10. (L) In wt, BN forms a tight bundle through its entire length. (N) In embryos carrying two copies of GMR-*Dscam* individual axons migrate aberrantly over the surface of the optic lobe. The position of the bo and the proximal region of the nerve appear normal. (M and O) High-magnification views of the optic lobe region stained with mAb22C10 (green) and anti-Bsh (red). (M) In wt, BN remains bundled and contacts P2. (O) Most axons mistarget (arrow) and do not contact P2 in embryos carrying one copy of GMR-*Dscam*. Scale bars: (A–H), 36 μm; (L and N), 14 μm; (M and O), 8 μm.

Dscam Interacts Genetically with *dock* and *Pak*

We sought to assess through genetic analysis whether *dock* and *Pak* are functional components of a *Dscam* guidance pathway. Mistargeting defects of BN were observed in some 44% of the embryos heterozygous for both *Dscam* and *dock* (Figure 7). In contrast, only 4%–6% and 10%–13% of embryos heterozygous for either *dock* or *Dscam*, respectively, showed defects. Similarly, whereas some 38% of BN were abnormal in embryos heterozygous for both *Dscam* and *Pak*, only 5% were defective in embryos heterozygous for *Pak*.

The synergistic interactions between *Dscam, dock*,

Table 1. Quantification of Pathfinding Defects in BN

Genotype	Complete Mistargeting (N)	Partial Mistargeting (N)	BN Analyzed (N)	Mistargeting (%)
$Dscam^{E1}/Df(2R)EW60$	19	22	78	53%
$Dscam^{E1}/Df(2R)cos\text{-}2$	28	20	89	54%
$Dscam^{P}/Df(2R)EW60$	20	30	94	53%
$Dscam^{P}/Df(2R)cos\text{-}2$	29	22	88	58%
$dock^{P2}/dock^{P1}$	53	52	109	96%
$dock^{3}/dock^{3}$	60	66	137	92%
Pak^{6}/Pak^{11}	31	49	89	90%
$dock^{P1}/dock^{P2}$; pGMR-dock	3	8	74	15%

Complete mistargeting indicates that the entire BN mistargets (see Figures 6C, 6E, and 6G). Partial mistargeting indicates that not all BN axons mistarget (see Figures 6D, 6F, and 6H).

Genotype	Complete mistargeting (N)	Partial mistargeting (N)	BN analysed (N)	Mistargeting (%)
dock^{3}/+	0	5	127	4%
dock^{P1}/+	0	4	61	6%
Pak^{6}/+	1	4	95	5%
Dscam^{P}/+	1	9	95	10%
Dscam$^{Df(2R)EW60}$/+	2	5	52	13%
Dscam^{P}/+ *dock*^{3}/+	20	34	128	42%
Dscam$^{Df(2R)EW60}$/+ *dock*^{3}/+	16	22	86	44%
Dscam^{P}/+; *Pak*^{6}/+	5	20	65	38%

Figure 7. *Dscam* Genetically Interacts with *dock* and *Pak*

Complete mistargeting indicates that the entire BN mistargets. Partial mistargeting indicates that not all BN axons mistarget. Examples of phenotypes observed are color coded to match the table. The BN projection was visualized using mAb22C10 (arrow) and anti-Bsh (arrowhead). An example of complete mistargeting is shown for an embryo heterozygous for both *Dscam* and *dock* and an example of partial mistargeting is shown for embryos heterozygous for *Dscam* and *Pak*.

and *Pak*, the similarity of complete loss-of-function phenotypes, and the physical interactions between these proteins are consistent with them acting together to mediate recognition between the BN growth cones and P2.

Multiple Forms of Dscam Are Generated by Alternative Splicing

Extensive cDNA analyses revealed alternative amino acid sequences for Ig domains 2, 3, 7, and the transmembrane domain (Figures 8 and 9). Alternative forms of each Ig domain were used to identify additional related sequences within the gene. This led to the identification of a total of 12, 48, and 33 potential alternative sequences for Ig2, Ig3, and Ig7, respectively (Figure 9). Two alternative transmembrane domains also were identified. The N-terminal half of Ig2 is encoded by alternative forms of exon 4, the N-terminal half of Ig3 is encoded by alternative forms of exon 6, and the entire Ig7 domain is encoded by alternative forms of exon 9. Exons are used in a mutually exclusive fashion. That is, each cDNA sequence contains only one each of the variable exons encoding Ig2, Ig3, and Ig7 and contains only one of the two alternative transmembrane domains. The protein sequences of alternative exons form highly related families (Figure 9): exons 4 share between 33% and 81% identity, exons 6 (with the exception of exon 6.11) share between 22% and 87% identity, exons 9 share between 23% and 92% identity, and the two alternative transmembrane segments share 25% identity.

The *Dscam* gene extends 61,206 nucleotides from the 5′ end of exon 1 to the poly(A) addition site in exon 24. Alternative forms of exon 4 are tandemly arranged within 6.5 kb of DNA between invariant exons 3 and 5, alternative forms of exon 6 within 12.7 kb flanked by invariant exons 5 and 7, and finally, the entire Ig7 domain is encoded by alternative exons in 15.7 kb of DNA bracketed by invariant exons 8 and 10. Alternative exons are flanked by conserved splice donor and acceptor sites. Regulatory sequences required for DNA rearrangement of sequences in the mammalian immune system were not identified. These observations support the notion that multiple forms of Dscam are generated by alternative splicing.

If alternative exons can be spliced independently, then the *Dscam* locus potentially encodes 38,016 isoforms. To gain some additional clues as to the number of alternative exons used and the variety of different combinations, we sequenced a panel of 50 cDNAs synthesized by RT-PCR prepared from mRNA isolated from 12–24 hr embryos. Inserts were 1.8 kb in length and spanned exons 3 through 10. Of these 50 cDNAs, 49 contained unique combinations of variable exons. Representatives of 11 of 12 exons 4, 30 of 48 exons 6, and 25 of 33 exons 9 were found in these cDNAs (Figure 8). Sequencing of other cDNAs from embryos and pupae revealed that an additional 1, 6, and 3 alternatives for exons 4, 6, and 9, respectively, were used (data not shown). These data suggest that all alternative exons are utilized in vivo.

A. *Dscam* contains constant and variable exons.

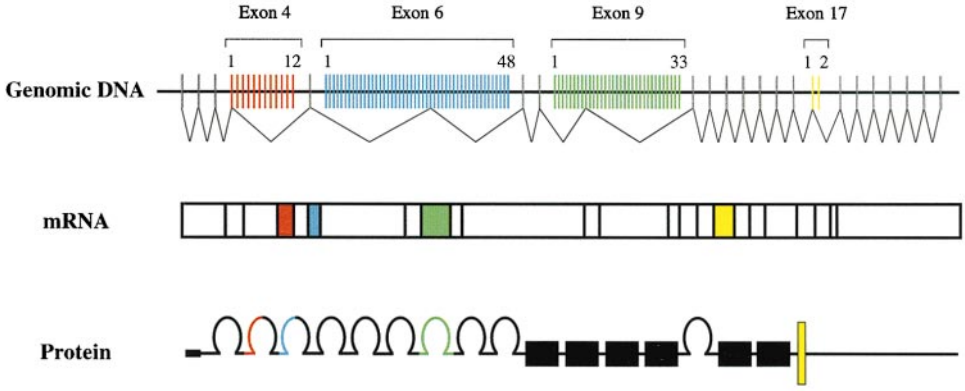

B. Differential use of alternative exons generates enormous receptor diversity.

cDNAs	Alternative Exons Observed: Exon 4	Exon 6	Exon 9
1	1	2	14
2	1	5	5
3	1	8	11
4	1	33	20
5	1	43	20
6	2	4	13
7	2	18	30
8	2	25	8
9	2	28	13
10	2	37	30
11	2	39	13
12	3	3	13
13	3	3	32
14	3	15	13
15	3	23	7
16	3	24	13
17	3	37	19
18	4	30	4
19	4	42	32
20	4	46	8
21	5	6	8
22	5	21	2
23	5	26	19
24	5	26	19
25	6	19	18

cDNAs	Alternative Exons Observed: Exon 4	Exon 6	Exon 9
26	6	27	16
27	6	30	17
28	6	34	7
29	6	36	16
30	6	37	23
31	7	6	5
32	7	7	12
33	7	18	5
34	7	19	21
35	7	20	9
36	7	24	1
37	7	42	8
38	8	4	26
39	8	6	16
40	8	19	15
41	8	30	25
42	8	48	24
43	9	35	3
44	10	16	2
45	10	37	14
46	10	42	25
47	10	48	26
48	12	7	16
49	12	15	16
50	12	18	9

Figure 8. Multiple Forms of Dscam Are Generated by Alternative Splicing

(A) The *Dscam* gene spans 61.2 kb of genomic DNA. Dscam mRNA extends 7.8 kb and comprises 24 exons. Mutually exclusive alternative splicing occurs for exons 4, 6, 9, and 17. 1 of 12 exon 4 alternatives, 1 of 48 exon 6 alternatives, 1 of 33 exon 9 alternatives, and 1 of 2 exon 17 alternatives are retained in each mRNA, as deduced from cDNA sequence. Variable exons are shown in color: exon 4, red; exon 6, blue; exon 9, green; and exon 17, yellow. Constant exons are represented by gray lines in genomic DNA and white boxes in mRNA. The splicing pattern shown (4.1, 6.28, 9.9, 17.1) corresponds to that obtained in the initial cDNA clone from S2 cells. The alternatively spliced exons 4, 6, 9, and 17 encode the N-terminal half of Ig2 (red), the N-terminal half of Ig3 (blue), the entire Ig7 (green), and the transmembrane domain (yellow), respectively.

(B) Alternative exons are expressed. RT-PCR was performed on total RNA isolated from 12–24 hr embryos. Fifty individual cDNA clones (numbers 1–50) were isolated and sequenced across exons 4, 6, and 9 (see Experimental Procedures). Alternative exons used in each cDNA are indicated. Color coding of exons in schematic corresponds to scheme in (A). 49 of the 50 cDNAs contain unique combinations of alternative exons.

Discussion

In this paper, we identified *Drosophila* Dscam, presented evidence that it is a guidance receptor, and reported the existence of multiple alternative forms. Through analysis of mutant embryos, we demonstrated that Dscam is required in BN for pathfinding to an intermediate target. Defects in axonal organization were also observed in the central nervous system in *Dscam* mutants. Several observations are consistent with Dscam

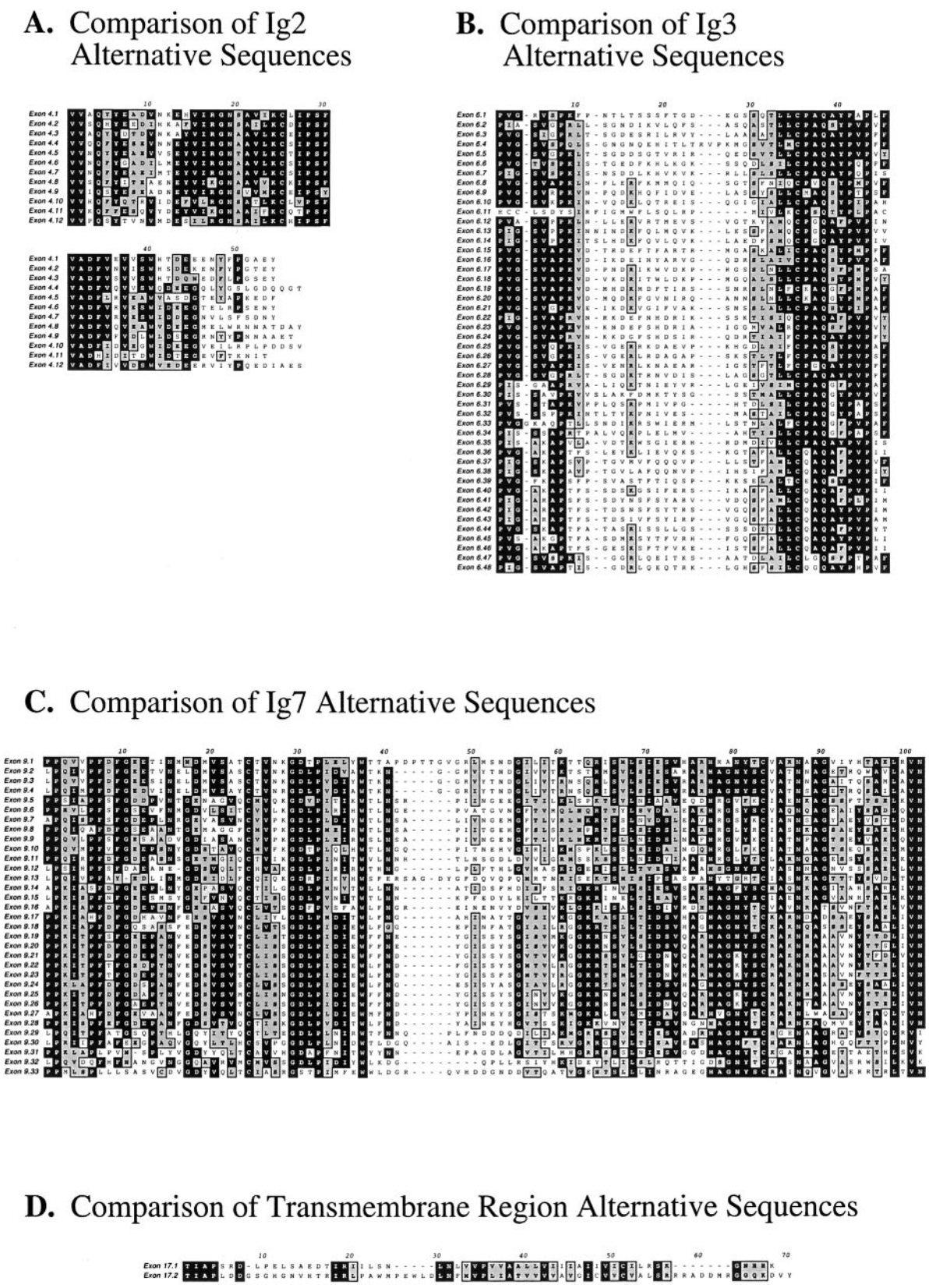

Figure 9. Sequence Alignments of Dscam Variable Domains

Alignments of the amino acid sequences encoded by variable exons 4 (A), 6 (B), 9 (C) and 17 (D). Alternative exons 4, 6, and 9 encode the N-terminal half of Ig2, the N-terminal half of Ig3, and the entire Ig7, respectively. Alternative exons 17 encode transmembrane domains and surrounding sequences. Dark shading represents sequence identity. Light shading represents sequence similarity.

acting as a guidance receptor directly upstream of Dock and Pak. First, Dscam and Pak physically interact with Dock. Second, *Dscam*, *dock*, and *Pak* BN phenotypes are similar. And finally, *Dscam* genetically interacts with both *dock* and *Pak*.

Korenberg and colleagues discovered human DSCAM and proposed that *DSCAM* trisomy contributes to the pathogenesis in brain development in Down syndrome patients (Yamakawa et al., 1998). Interestingly, overexpression of *Drosophila* Dscam selectively in BN leads to a strong dominant defect in axon guidance. Whether this is caused by an increased level of Dscam in the growth cone or expression of an inappropriate isoform remains unclear. It is important to note, however, that overexpression in this system is likely to exceed the increased level of expression associated with trisomy. That neurons may be particularly sensitive to *Dscam* dosage is suggested further by the finding that some 10%–13% of embryos heterozygous for *Dscam* show defects in BN axon guidance. Identification of the specific isoforms normally expressed in BN and the modulation of these levels may provide further clues as whether modest increases in Dscam levels promote defects in neural development.

Dscam Acts with Dock and Pak to Transmit Guidance Signals

We envision that during BN guidance a signal from P2, an intermediate target, attracts BN growth cones. In *dock*, *Pak*, and *Dscam* mutants, BN frequently comes in close proximity to P2 and projects past it or deflects away from it. Hence, we favor the view that Dscam plays a prominent role in recognizing a local attractive signal at P2. As the *Dscam* phenotype in the CNS is more severe than that of *dock* (Desai et al., 1999), it is likely that Dscam also functions through other downstream components in other neurons.

How might binding of Dscam on a filopodial process to a ligand at P2 promote attraction? We propose two alternative models. First, Dock and Dscam may form a complex in the absence of ligand. This interaction would be mediated by the SH3-1 and SH3-3 domains in Dock and two closely spaced PXXP sites in Dscam's cytoplasmic tail. Dock's SH3-2 domain may bind to the polyproline stretch in the C-terminal tail; this may prevent recruitment of Pak to the membrane in the absence of ligand. Upon encountering an attractive ligand at P2, however, we envision that Dscam becomes tyrosine phosphorylated. This may promote rearrangement of the complex with Dock binding through its SH2 domain to phosphotyrosine. This conformational change cannot strictly depend upon the SH2 domain, as the SH3-1 and SH3-3 domains can functionally compensate for the SH2 domain (Rao and Zipursky, 1998). This conformational change would unmask the SH3-2 domain, thus facilitating recruitment of Pak to the complex. Pak, in turn, would promote actin reorganization and subsequent movement of the growth cone to P2. Alternatively, in the absence of ligand the cytoplasmic tail of Dscam may be in a conformation not accessible to Dock binding. In this model, ligand binding would promote both a conformational change in Dscam's cytoplasmic domain and tyrosine phosphorylation. Dock may then associate with Dscam and recruit Pak to the membrane. Candidates for additional components in this signaling pathway have been identified through biochemical and genetic studies and include a nonreceptor tyrosine kinase, an adaptor protein linked to actin, and a nonreceptor tyrosine phosphatase (Clemens et al., 1996; J. C. C. et al., unpublished data). A precise mechanistic understanding of the relationship between Dscam, Dock, and Pak and these additional components will require identification of the Dscam ligand and detailed biochemical studies.

Does human DSCAM signal through Nck and Pak? While the extracellular region of human and *Drosophila* Dscam share identical domain structures and highly related amino acid sequences, the intracellular domains appear unrelated. This may indicate that the human and fly proteins signal downstream via different pathways or that the interactions with Nck are mediated by other proline-rich sequences, phosphotyrosine residues or other associated proteins. Alternatively, there may be multiple mammalian DSCAM genes, one of which shares sequence homology with the cytoplasmic domain of the fly protein. While a partial sequence of a second DSCAM-related gene has been identified on human chromosome 11 (accession no. BAA86446), its cytoplasmic domain is conserved with human DSCAM and is unrelated to *Drosophila* Dscam.

Multiple Isoforms of Dscam May Contribute to Connection Specificity

Through sequence analysis of cDNAs, we uncovered multiple forms of Dscam. These different forms encode proteins with the same architecture but with sequence variations in three different Ig domains and the transmembrane domain. Genomic analysis revealed that exons encoding these alternative domains are tandemly arranged. There are 12 alternative forms of exon 4 (encoding the N-terminal half of Ig2), 48 alternative forms of exon 6 (encoding the N-terminal half of Ig3), 33 alternative forms of exon 9 (encoding Ig7), and 2 alternative forms of exon 17 (encoding transmembrane domains). DNA sequence analysis supports the view that multiple forms of Dscam are generated by alternative splicing. If all combinations are permissible, 38,016 forms of Dscam may be generated. This level of diversity is comparable to that achieved in individual antibody protein subunits through rearrangement prior to further diversification via TdT-mediated nucleotide insertion and somatic mutation. For instance, it is estimated that in human recombination generates some 9,180 variable heavy chains (51 VH segments, 30 D segments and 6 J segments) (Cook and Tomlinson, 1995). Our analysis revealed that an extraordinary diversity of Dscam isoforms is expressed during development. As the mechanisms utilized to generate splicing of one of two alternative exons, in many other well-characterized genes, are poorly understood (Lopez, 1998), it seems premature to entertain models for the molecular mechanisms regulating the "either–or" splicing patterns for the 12, 48, and 33 densely packed alternative exons in *Dscam*. We have not observed alternative forms of human DSCAM in searches of available genomic sequences and ESTs. Hence, either alternatively spliced forms of DSCAM are not generated in

mammals or diversity exists among DSCAM-related genes.

Several other cell surface proteins involved in neuronal connectivity or implicated in the process show considerable molecular diversity. The vertebrate olfactory receptors, encoded by a large gene family containing in excess of 1000 different sequences, play a key role in determining glomerular specificity in the olfactory bulb, although they do not appear to be the sole specificity determinants (Wang et al., 1998). Multiple forms of neurexins also have been proposed to play a role in synapse specificity (see Missler and Südhof, 1998). Alternative splicing of neurexins encoded by three different genes may give rise to more than a 1000 different isoforms differing in size and amino acid sequence. In contrast to neurexins, all Dscam isoforms share a common domain architecture. While loss-of-function studies have not yet critically addressed the role of neurexins in forming neuronal connections, their localization to synapses makes them intriguing candidates for contributing to connection specificity.

Two cadherin cell adhesion molecule subfamilies containing multiple forms also have been implicated in specificity (for review see Uemura, 1998). There are some 20 different classic cadherins expressed in mammals. They are localized to synapses and, in some cases, show restricted patterns of expression correlating with specific functional pathways (Takeichi et al., 1997; Shapiro and Colman, 1999). Recently, a second family of cadherins, cadherin-related neuronal receptors (CNRs), was identified in mice through a protein interaction screen and were shown to be expressed at synapses (Kohmura et al., 1998). Fifty-two different forms of CNRs have been identified in three different clusters in the human genome (Wu and Maniatis, 1999). The mRNAs encoding the mouse CNRs are expressed in a diffuse and rather general pattern within the nervous system. In the olfactory bulb, two different CNRs were shown to be coexpressed in a single neuron while a smaller fraction of neurons expressed only one or the other CNR. This raises the intriguing possibility that different combinations of CNRs in different neurons could impart connection specificity (Serafini, 1999). Given the conservation between guidance receptors in flies and mammals, it is surprising that CNRs were not identified in the recently published DNA sequence of the *Drosophila* genome (Rubin et al., 2000). While it is still unclear whether DSCAM-related genes in mammals may be alternatively spliced, different organisms may have evolved different strategies to generate diversity among related guidance receptors, as a means of specifying complex patterns of neuronal connectivity.

To our knowledge, the massive use of alternative exons in a combinatorial fashion to generate thousands of different protein isoforms all sharing a common architecture with differences in amino acid sequence is unprecedented within the nervous system. The physiological importance of these different isoforms remains entirely unclear. Diverse forms of Dscam may recognize distinct isoforms of specific ligands. That such alterations could lead to changes in ligand–receptor interaction are supported by the findings that alternative forms of Ig repeats in murine FGF receptor 1, generated by alternative splicing, exhibit marked differences in affinity for bFGF (Werner et al., 1992). Alternatively, Dscam may form dimers with other forms of Dscam or act as coreceptors to modulate the activities of other guidance receptors. In this context, it is interesting to note that Goodman and colleagues (Winberg et al., 1998) have proposed that accurate targeting of motoneurons to their specific muscle targets requires input from multiple receptor pathways. Future studies will identify proteins binding to the extracellular domain of Dscam, address whether different forms of Dscam are expressed in specific neurons, and test the functional importance of diversity.

Experimental Procedures

Cell Culture and RNAi

S2 cells were propagated as previously described (Clemens et al., 1996). A cDNA encoding a histidine-tagged (6× histidine) SH2 domain ($S2^{HisSH2}$) of Dock was inserted into pAT-Hygro, transfected into S2 cells, and selected (Herbst et al., 1996), producing the $S2^{HisSH2}$ cell line. For RNAi, a PCR fragment (700 bp) containing coding sequence for Dscam was used to produce double-stranded RNA as described (Clemens et al., 2000).

Purification of p270

$S2^{HisSH2}$ cells (6×10^{10}) were harvested by centrifugation and suspended in lysis buffer (100 ml; 50 mM Tris, pH 8.0, 500 mM KCl, 150 mM NaCl, 2 mM sodium vanadate, 10 mM NaF, 1% NP-40, 10% glycerol, 10 mM imidazole, 1× complete EDTA-free protease inhibitors [Roche]). Cells were lysed using a PT-2000 polytron (Kinematica). The lysate was cleared by centrifugation (27,000 × g), and incubated with gentle rocking with Ni-Agarose in lysis buffer (7 ml). The resin was washed with lysis buffer (3 × 40 ml), lysis buffer lacking KCl (2 × 40 ml), and eluted (7.5 ml; low salt buffer plus 200 mM imidazole). SDS (800 μl; 10%) was added to the eluent and boiled (5 min). RIPA buffer (80 ml) (Clemens et al., 1996) lacking SDS was added to the boiled eluate and incubated (16 hr) with 4G10 anti-phosphotyrosine resin (1 ml). 4G10 resin was washed with RIPA buffer (10 ml; including SDS) followed by 100 mM triethylamine (TEA) (10 ml; pH 8.0). Proteins were eluted in TEA (10 ml; pH 11.5). Eluted proteins were dried, dissolved in SDS-PAGE loading buffer (20 μl), boiled (5 min), and separated by SDS-PAGE (7.5%). A p270 band was visualized by Coomassie staining, excised for tryptic digestion, and microsequenced (Harvard Microchem).

Molecular Analysis of Dscam

EST clones were obtained from the Berkeley Drosophila Genome Project (BDGP). Other cDNA clones were obtained from various cDNA libraries. cDNA sequences were aligned to a DNA contig from Celera and BDGP using the BDGP BLAST server. Additional sequence analysis was done using MacVector ClustalW alignments (Oxford Molecular Group) and a splice site prediction program (BDGP). Details available upon request. To obtain clone sequences reported in Figure 7B, reverse transcription was performed on total RNA isolated from 12–24 hr embryos. First strand synthesis was primed using an exon 11 primer. PCR was performed using primers from exons 3 and 11. A 2.4 kb product was cut with BamHI and cloned into pBluescript (Stratagene). Individual clones were isolated and sequenced using T7 and T3 primers and an internal primer in exon 7.

Characterization of Interactions between Dscam and Dock

The small-scale purification procedure of SH2-associated proteins was a modified version of the large scale purification (see above). Immune precipitation from embryos and S2 cells was carried out essentially as previously described (Clemens et al., 1996). Gel-overlay analysis was performed by radiolabeling recombinant GST-DockSH2, probing, and washing essentially as described (Margolis and Young, 1995). Dock binding experiments with proteins transcribed and translated in vitro were a modified version of Tang et al. (2000). Mutations were introduced into the cytoplasmic domain

of Dscam using the QuikChange Site-Directed Mutagenesis Kit from Stratagene. Primers were designed to change P1685 and P1686 into leucines in P1L and P1,2L, while P1727 and P1728 were changed to leucine and threonine, respectively, in P2L and P1,2L.

Yeast Two-Hybrid Assay

Yeast two-hybrid assays were performed as previously described (Hing et al., 1999). The Dscam cytoplasmic domain (aa 1657–2016), the C-terminal part of the cytoplasmic domain (aa 1817–2016), and various mutant forms were fused to the yeast Gal4 activation domain (pGAD424). β-galactosidase activity (Miller units) was represented qualitatively: −, less than 1 unit; +, 1–10 units; ++, 11–20 units; +++++, more than 40 units.

Genetics

For description of *dock* and *Pak* mutations, see Garrity et al. (1996) and Hing et al. (1999). For deficiencies and mutations of the 43B region see Heitzler et al. (1993). The P element insertion in $Dscam^{P}$ was mapped by sequence analysis of a plasmid rescue fragment (O'Kane, 1998). Polytene chromosomes from wild-type, *Df(2R)CA68*/+, and *Df(2R)drl21*/+ larvae were used for in situ hybridization (Pardue, 1994). Bolwig's organ–specific expression of Dscam was achieved by inserting a full-length Dscam cDNA (containing alternative exons 4.1, 6.30, 9.30, and 17.2) into the pGMR transformation vector and introducing into the germline by P element transformation. Two lines, one with an insertion on the X and the other on the second chromosome, were analyzed. Expression of the Dscam protein in these lines was confirmed by anti-Dscam antibody staining. To assess rescue, homozygous embryos from the cross $dock^{P1}$/*CyO GFP*; *pGMR-dock* and $dock^{P2}$/*CyO GFP* were analyzed for BN defects as described in results.

Immunohistology

Primary antibodies used for immunohistochemistry were: rabbit anti-Dscam (1:300); mAb22C10 (Fujita et al., 1982; 1:50); guinea pig anti-Bsh (1:750); rabbit anti β-galactosidase (Cappel; 1:1000); rabbit anti-Krüppel (Hoch et al., 1994; 1:500); mAb BP102 (Seeger et al., 1993; 1:10); and mAb 1D4 anti-Fas II (Van Vactor et al., 1993; 1:50). Immunohistochemistry and mounting of embryos were carried out as described by Schmucker et al. (1997). Fluorescent samples were analyzed using a Bio-Rad MRC 1024 confocal microscope. In situ hybridization of Dscam was achieved using DIG-labeled riboprobes as described by Sheng et al. (1997).

Acknowledgments

We thank Utpal Banerjee, Eddy De Robertis, Gerry Weinmaster, Owen Witte, and members of the Zipursky lab for comments on the manuscript, Dorian Gunning and Nancy Simonson-Leff for superb technical assistance, Karen Ronan for help in preparing the manuscript, and Pascal Heitzler for mutant flies. We would also like to thank Doug Black, Ben Margolis, Julie Korenberg, Corey Goodman, and Marc Tessier-Lavigne for helpful discussions. This work was supported by HFSPO and Max Planck Society Fellowships (D. S.), an NIH Training Grant in Biotechnology (J. X.), MSTP NIH grant #GM08042 (H. S.), the Walther Cancer Institute (J. E. D.), and grants from the NIH (J. E. D.). S. L. Z. is an Investigator of the Howard Hughes Medical Institute.

Received April 14, 2000; revised April 28, 2000.

References

Albright, T.D., Jessell, T.M., Kandel, E.R., and Posner, M.I. (2000). Neural science: a century of progress and the mysteries that remain. Cell Suppl. *100*, S1–S55.

Bashaw, G.J., and Goodman, C.S. (1999). Chimeric axon guidance receptors: the cytoplasmic domains of slit and netrin receptors specify attraction versus repulsion. Cell *97*, 917–926.

Clemens, J.C., Ursuliak, Z., Clemens, K.K., Price, J.V., and Dixon, J. (1996). A Drosophila protein-tyrosine phosphatase associates with an adapter protein required for axonal guidance. J. Biol. Chem. *271*, 17002–17005.

Clemens, J.C., Worby, C.A., Simonson-Leff, N., Muda, M., Maehama, T., Hemmings, B.A., and Dixon, J.E. (2000). Use of double-stranded RNA interference in Drosophila cell lines to dissect signal transduction pathways. Proc. Natl. Acad. Sci. USA, in press.

Cook, G.P., and Tomlinson, I.M. (1995). The human immunoglobulin VH repertoire. Immunol. Today *16*, 237–242.

Culotti, J.G., and Merz, D.C. (1998). DCC and netrins. Curr. Opin. Cell Biol. *10*, 609–613.

Desai, C.J., Garrity, P.A., Keshishian, H., Zipursky, S.L., and Zinn, K. (1999). The Drosophila SH2-SH3 adapter protein Dock is expressed in embryonic axons and facilitates synapse formation by the RP3 motoneuron. Development *126*, 1527–1535.

Flanagan, J.G., and Vanderhaeghen, P. (1998). The ephrins and Eph receptors in neural development. Annu. Rev. Neurosci. *21*, 309–345.

Fujita, S.C., Zipursky, S.L., Benzer, S., Ferrus, A., and Shotwell, S.L. (1982). Monoclonal antibodies against the Drosophila nervous system. Proc. Natl. Acad. Sci. USA *79*, 7929–7933.

Garrity, P.A., Rao, Y., Salecker, I., McGlade, J., Pawson, T., and Zipursky, S.L. (1996). Drosophila photoreceptor axon guidance and targeting requires the Dreadlocks SH2/SH3 adapter protein. Cell *85*, 639–650.

Goodman, C.S., and Shatz, C.J. (1993). Developmental mechanisms that generate precise patterns of neuronal connectivity. Cell Suppl. *72*, 77–98.

Guthrie, S. (1999). Axon guidance: starting and stopping with slit. Curr. Biol. *9*, R432–R435.

Hall, A. (1998). Rho GTPases and the actin cytoskeleton. Science *279*, 509–514.

Heitzler, P., Coulson, D., Saenz-Robles, M.T., Ashburner, M., Roote, J., Simpson, P., and Gubb, D. (1993). Genetic and cytogenetic analysis of the 43A-E region containing the segment polarity gene costal and the cellular polarity genes prickle and spiny-legs in Drosophila melanogaster. Genetics *135*, 105–115.

Herbst, R., Carroll, P.M., Allard, J.D., Schilling, J., Raabe, T., and Simon, M.A. (1996). Daughter of sevenless is a substrate of the phosphotyrosine phosphatase Corkscrew and functions during sevenless signaling. Cell *85*, 899–909.

Hing, H., Xiao, J., Harden, N., Lim, L., and Zipursky, S.L. (1999). Pak functions downstream of Dock to regulate photoreceptor axon guidance in Drosophila. Cell *97*, 853–863.

Hoch, M., Broadie, K., Jäckle, H., and Skaer, H. (1994). Sequential fates in a single cell are established by the neurogenic cascade in the Malpighian tubules of Drosophila. Development *120*, 3439–3450.

Hong, K., Hinck, L., Nishiyama, M., Poo, M.M., Tessier-Lavigne, M., and Stein, E. (1999). A ligand-gated association between cytoplasmic domains of UNC5 and DCC family receptors converts netrin-induced growth cone attraction to repulsion. Cell *97*, 927–941.

Kidd, T., Brose, K., Mitchell, K.J., Fetter, R.D., Tessier-Lavigne, M., Goodman, C.S., and Tear, G. (1998). Roundabout controls axon crossing of the CNS midline and defines a novel subfamily of evolutionarily conserved guidance receptors. Cell *92*, 205–215.

Kohmura, N., Senzaki, K., Hamada, S., Kai, N., Yasuda, R., Watanabe, M., Ishii, H., Yasuda, M., Mishina, M., and Yagi, T. (1998). Diversity revealed by a novel family of cadherins expressed in neurons at a synaptic complex. Neuron *20*, 1137–1151.

Kolodziej, P.A., Timpe, L.C., Mitchell, K.J., Fried, S.R., Goodman, C.S., Jan, L.Y., and Jan, Y.N. (1996). *frazzled* encodes a Drosophila member of the DCC immunoglobulin subfamily and is required for CNS and motor axon guidance. Cell *87*, 197–204.

Lance-Jones, C., and Landmesser, L. (1981). Pathway selection by chick lumbosacral motoneurons during normal development. Proc. R. Soc. London B Biol. Sci. *214*, 1–18.

Lin, C.H., and Forscher, P. (1993). Cytoskeletal remodeling during growth cone-target interactions. J. Cell Biol. *121*, 1369–1383.

Lopez, A.J. (1998). Alternative splicing of pre-mRNA: Developmental consequences and mechanisms of regulation. Annu. Rev. Genet. *32*, 279–305.

Manser, E., Leung, T., Salihuddin, H., Zhao, Z.-S., and Lim, L. (1994). A brain serine/threonine protein kinase activated by Cdc42 and Rac1. Nature *367*, 40–46.

Margolis, B., and Young, R.A. (1995). DNA Cloning: A Practical Approach, Second Edition, D.N. Glover and B.D. Hames, eds. (Oxford: IRL Press), pp. 1–14.

Ming, G.L., Song, H.-J., Berninger, B., Holt, C.E., Tessier-Lavigne, M., and Poo, M.-M. (1997). cAMP-dependent growth cone guidance by netrin-1. Neuron *19*, 1225–1235.

Missler, M., and Südhof, T.C. (1998). Neurexins: three genes and 1001 products. Trends Genet. *14*, 20–26.

Nobes, C.D., and Hall, A. (1995). Rho, rac, and cdc42 GTPases regulate the assembly of multimolecular focal complexes associated with actin stress fibers, lamellipodia and filopodia. Cell *81*, 53–62.

O'Kane, C.J. (1998). Enhancer traps. In Drosophila: A Practical Approach, D.B. Roberts, ed. (Oxford: IRL Press), pp. 139–178.

Olivier, J.P., Raabe, T., Henkemeyer, M., Dickson, B., Mbamalu, G., Margolis, B., Schlessinger, J., Hafen, E., and Pawson, T. (1993). A Drosophila SH2-SH3 adaptor protein implicated in coupling the sevenless tyrosine kinase to an activator of Ras guanine nucleotide exchange, Sos. Cell *73*, 179–191.

Pardue, M.-L. (1994). Looking at polytene chromosomes. In Drosophila melanogaster: Practical Uses in Cell and Molecular Biology, E.A. Fyrberg and L.S.B. Goldstein, eds. (San Diego, CA: Academic Press), pp. 334–353.

Rao, Y., and Zipursky, S.L. (1998). Domain requirements for the Dock adapter protein in growth-cone signaling. Proc. Natl. Acad. Sci. USA *95*, 2077–2082.

Rubin, G.M., Yandell, M.D., Wortman, J.R., Gabor Miklos, G.L., Nelson, C.R., Hariharan, I.K., Fortini, M.E., Li, P.W., Apweiler, R., Fleischmann, W., et al. (2000). Comparative genomics of the eukaryotes. Science *287*, 2204–2215.

Schmucker, D., Jäckle, H., and Gaul, U. (1997). Genetic analysis of the larval optic nerve projection in Drosophila. Development *124*, 937–948.

Schultz, J., Copley, R.R., Doerks, T., Ponting, C.P., and Bork, P. (2000). SMART: a web-based tool for the study of genetically mobile domains. Nucleic Acids Res. *28*, 231–234.

Seeger, M., Tear, G., Ferres-Marco, D., and Goodman, C.S. (1993). Mutations affecting growth cone guidance in Drosophila: genes necessary for guidance toward or away from the midline. Neuron *10*, 409–426.

Serafini, T. (1999). Finding a partner in a crowd: neuronal diversity and synaptogenesis. Cell *98*, 133–136.

Shapiro, L., and Colman, D.R. (1999). The diversity of cadherins and implications for a synaptic adhesive code in the CNS. Neuron *23*, 427–430.

Sheng, G., Thouvenot, E., Schmucker, D., Wilson, D.S., and Desplan, C. (1997). Direct regulation of rhodopsin 1 by Pax-6/eyeless in Drosophila: evidence for a conserved function in photoreceptors. Genes Dev. *11*, 1122–1131.

Song, H.J., Ming, G.-L., He, Z., Lehmann, M., Mckerracher, L., Tessier-Lavigne, M., and Poo, M.-M. (1998). Conversion of neuronal growth cone responses from repulsion to attraction by cyclic nucleotides. Science *281*, 1515–1518.

Stein, E., Huynh-Do, U., Lane, A.A., Cerretti, D.P., and Daniel, T.O. (1998). Nck recruitment to Eph receptor, EphB1/ELK, couples ligand activation to c-Jun kinase. J. Biol. Chem. *273*, 1303–1308.

Suter, D.M., and Forscher, P. (1998). An emerging link between cytoskeletal dynamics and cell adhesion molecules in growth cone guidance. Curr. Opin. Neurobiol. *8*, 106–116.

Takeichi, M., Uemura, T., Iwai, Y., Uchida, N., Inoue, T., Tanaka, T., and Suzuki, S.C. (1997). Cadherins in brain patterning and neural network formation. Cold Spring Harb. Symp. Quant. Biol. *62*, 505–510.

Tanaka, E., and Sabry, J. (1995). Making the connection: cytoskeletal rearrangements during growth cone guidance. Cell *83*, 171–176.

Tang, J., Kao, P.N. and Herschman, H.R. (2000). Protein arginine methyltransferase I (PRMT1), the predominant protein arginine methyltransferase in cells, interacts with and is regulated by interleukin enhancing binding factor 3. J. Biol. Chem., in press.

Tessier-Lavigne, M., and Goodman, C.S. (1996). The molecular biology of axon guidance. Science *274*, 1123–1133.

Thomas, J.B., Bastiani, M.J., Bate, M., and Goodman, C.S. (1984). From grasshopper to Drosophila: a common plan for neuronal development. Nature *310*, 203–207.

Uemura, T. (1998). The cadherin superfamily at the synapse: more members, more missions. Cell *93*, 1095–1098.

Van Vactor, D., Sink, H., Fambrough, D., Tsoo, R., and Goodman, C.S. (1993). Genes that control neuromuscular specificity in Drosophila. Cell *73*, 1137–1153.

Wang, F., Nemes, A., Mendelsohn, M., and Axel, R. (1998). Odorant receptors govern the formation of a precise topographic map. Cell *93*, 47–60.

Werner, S., Duan, D.R., De Vries, C., Peters, K.G., Johnson, D.E., and Williams, L.T. (1992). Differential splicing in the extracellular region of fibroblast growth factor receptor I generates receptor variants with different ligand-binding specificities. Mol. Cell. Biol. *12*, 82–88.

Winberg, M.L., Mitchell, K.J., and Goodman, C.S. (1998). Genetic analysis of the mechanisms controlling target selection: complementary and combinatorial functions of netrins, semaphorins, and IgCAMs. Cell *93*, 581–591.

Wu, Q., and Maniatis, T. (1999). A striking organization of a large family of human neural cadherin-like cell adhesion genes. Cell *97*, 779–790.

Yamakawa, K., Huot, Y.K., Haendelt, M.A., Hubert, R., Chen, X.N., Lyons, G.E., and Korenberg, J.R. (1998). DSCAM: a novel member of the immunoglobulin superfamily maps in a Down syndrome region and is involved in the development of the nervous system. Hum. Mol. Genet. *7*, 227–237.

GenBank Accession Number

The *Dscam* gene, mRNA, and alternative exon sequences have been deposited in GenBank under the accession number AF260530.